Amino Acids (2015) 47:1225–1238
DOI 10.1007/s00726-015-1949-6

ORIGINAL ARTICLE

Metabolomic analysis reveals distinct profiles in the plasma and urine of rats fed a high-protein diet

Chunlong Mu · Yuxiang Yang · Zhen Luo · Weiyun Zhu

Received: 23 October 2014 / Accepted: 19 February 2015 / Published online: 20 March 2015

Abstract A high-protein, low-carbohydrate diet has been regarded as a dietary intervention for weight loss in the obese population. We integrated metabolomics profiles and correlation-based network analysis to reveal the difference in metabolism under diets with different protein:carbohydrate ratios. Rats were fed a control diet (moderate-protein moderate-carbohydrate: MPMC; 20 % protein, 56 % carbohydrate) or HPLC diet (high-protein low-carbohydrate: 45 % protein, 30 % carbohydrate) for 6 weeks. The fat content was equal for both diets. HPLC feeding induced weight loss and reduced adipose weight and plasma triglyceride. Compared to the MPMC diet, HPLC significantly increased plasma α-tocopherol, pyruvate, 2-oxoisocaproate, and β-hydroxybutyrate, and reduced linoleate, palmitate, α-glycerophosphate and pyroglutamic acid. The HPLC-associated urinary metabolite profile was signified with an increase in palmitate and stearate and a reduction of citrate, 2-ketoglutarate, malate, and pantothenate. Pathway analysis implicated a significant alteration of the TCA cycle in urine. Biomarker screening demonstrated that individual metabolites, including plasma urea, pyruvate, and urinary citrate, robustly distinguished the HPLC group from the MPMC group. Correlation-based network analysis enabled to demonstrate that the correlation of plasma metabolite was strengthened after the HPLC diet, while the energy-metabolism relatives 2-ketoglutarate and fumarate correlated positively with phenylalanine, methionine, and serine. The correlation network between plasma–urinary metabolites revealed a negative correlation of plasma valine with urinary β-hydroxybutyrate in MPMC rats. In HPLC rats, plasma 2-oxoisocaproate negatively correlated with urinary pyruvate and glycine. This study using metabolomics analysis revealed the systemic metabolism in response to diet treatment and identified the significantly distinct profiles associated with a HPLC diet.

Keyword Metabolomics profiling · Correlation network · High-protein low-carbohydrate diet · Rat

Handling Editor: F. Blachier.

C. Mu and Y. Yang contributed equally to this work.

Electronic supplementary material The online version of this article (doi:10.1007/s00726-015-1949-6) contains supplementary material, which is available to authorized users.

C. Mu · Y. Yang · Z. Luo · W. Zhu (✉)
Laboratory of Gastrointestinal Microbiology, College of Animal Science and Technology, Nanjing Agricultural University, Nanjing 210095, China
e-mail: zhuweiyun@njau.edu.cn

Introduction

A high-protein, low-carbohydrate (HPLC) diet has been demonstrated to display weight-loss effects in humans (Sacks et al. 2009) and rats (Jean et al. 2001). Previous studies have revealed multiple effects of a high-protein intake, such as decreased blood triglyceride and improved glycemic control in subjects with type 2 diabetes mellitus (Halton and Hu 2004). However, a high-protein diet has also been shown to lead to an increase in hazardous fecal N-nitroso compounds and a reduction in cancer-protective phenolic acids, which may be detrimental to human health (Russell et al. 2011). Recent studies have shown that as the protein:carbohydrate ratio increases, the death risk increases in mice (Solon-Biet et al. 2014). Thus, it is vital to understand the underlying mechanisms of the weight-loss effect and potential accompanying side-effects resulting from a high-protein diet, especially in terms of whole

body metabolism. Although a number of studies have been conducted to investigate weight-loss effects and metabolic alteration, little is known about the systemic metabolism effect.

Metabolomics profiling is useful when it comes to understanding dietary influences via urine analysis (Ross et al. 2013), and in identifying disease biomarkers by analyzing plasma (Schicho et al. 2012) or urine (Seyfried et al. 2013). Rasmussen et al. (2012) investigated the effect of a high-protein diet on urinary metabolic profiles in human adults and revealed that urinary creatinine increased while citric acid decreased after consuming high protein for 6 months. Furthermore, Reimer et al. (2012) reported the influence of an intermittent high-fat/sucrose diet during high-milk protein intake on rat plasma metabolites, and showed that switching dietary components resulted in an increase in plasma isobutyrate, mannose, leucine, and isoleucine and the reduction of creatinine, citrate, and serine in plasma. In addition, Deng et al. (2014) found that healthy adult cats fed with a HPLC diet showed an increase in amino acid (AA) metabolism and β-hydroxybutyrate (BHB), and a decrease in nucleotide catabolism. These studies have provided the first account for either urine or plasma metabolic profiles after a high-protein diet intake. However, to provide an overall view of the metabolic response to dietary invention, it is important to understand the metabolic change at the systemic level by simultaneously monitoring the metabolic profiles in both plasma and urine. Given that plasma and urinary metabolites reflect local absorption and systemic excretion, which is regulated by internal metabolic mechanisms, it is important to understand the potential metabolic relationship within plasma or between plasma and urinary metabolites.

In addition to monitoring the macroscopic changes in metabolite concentrations, metabolomics network analysis is able to reveal the metabolite correlation under specific experimental conditions. The statistical metabolite correlation may reflect the biological association between metabolites. Using computational modeling analysis in yeast, Camacho et al. (2005) demonstrated that several factors, such as chemical equilibrium and enzyme regulation, could lead to a high correlation between metabolite pairs that are neighbors in the metabolic network. In animal bodies, highly correlated signals are likely to come from the same metabolites or from metabolites regulated by the same metabolic pathway (Nicholson et al. 2012). Thus, metabolomics correlation analysis is important to explore metabolite correlation, which could complement our understanding of the potential biological regulation in rats under nutritional intervention.

In the present study, using a rat model, gas chromatography–mass spectrometry (GC/MS)-based metabolic profiling was adopted to explore the change of metabolites in plasma and urine in rats with normal weight or HPLC-induced weight loss. At systemic level, this study for the first time enabled to reveal distinct metabolic profiles in rats with HPLC diet. Network analysis showed abundant correlations between plasma metabolites and plasma–urine metabolites in MPMC or HPLC rats. The distinct metabolic profiles and correlation network change may enable to provide reference for the nutritional intervention on the basis of metabolic network regulation.

Methods and materials

Experimental design

The experiment was carried out in accordance with the Chinese guidelines for animal welfare. Experimental protocols are approved by the Ethical Committee of Nanjing Agricultural University, Nanjing, China. A total of 20 male Wistar rats weighing 180–200 g (Qinglongshan Animal Center, Nanjing, China) were maintained in individual cages with free access to water and under controlled conditions of temperature and humidity, with a 12-h:12-h light/dark cycle for 1 week before starting the experiment. Rats were fed with the standard diet (MPMC) during the acclimation. After the adaptation period, rats were then randomly allocated to two groups of 10 rats each ($n = 10$) and offered with isoenergetic standard diets either a casein-based MPMC (20 % protein, 56 % carbohydrate) or HPLC (45 % protein, 30 % carbohydrate) diet (Supplementary Table 1). The fat and fiber content were equal for both diets. Food residues were recorded daily and fresh food was provided at the end of the daily light period. Housing and growth environment were maintained during experimental periods. Rats were weighed three times weekly and health status was assessed twice daily by clinical monitoring, and no signs of illness were observed during the 6-week experiment.

Sampling collection

At the end of experiment (the 42nd day), rats fasting overnight were weighed and anesthetized with diethyl ether. Blood was collected from precaval vein, drawn into EDTA-coated tube and centrifuged for 10 min at 4 °C and 4000 rpm. The supernatant (plasma) samples were stored in aliquots at −80 °C until analysis. Urine samples were collected from vesica urinaria and stored in aliquots at −80 °C before analysis. Epididymal and mesenteric fat pads, liver and spleen were removed and weighed.

Biochemical measurements

Total protein, globulin, albumin, glucose, triglyceride, total cholesterol, high-density lipoprotein cholesterol (HDLC),

low-density lipoprotein cholesterol (LDLC), urea, creatinine and uric acid in plasma were determined by the enzymatic colorimetric method with Olympus AU2700 auto analyzer (Olympus, Tokyo, Japan). Glutamic-pyruvic transaminase (GPT) and glutamic-oxalacetic transaminase (GOT) activity were determined using Reitman and Frankel method (Reitman and Frankel 1957) on spectrophotometer (Multiskan GO 1.00.38, Vantaa, Finland). GPT and GOT were selected as markers for hepatocellular damage. Plasma concentrations of insulin, glucagon, triiodothyronine, thyroxine, gastrin and growth hormone were determined using radioimmunoassay kits with ^{125}I as a tracer (North Institute of Biological Technology, Beijing, China), according to the instruction of the manufacturer. Radioactivity of ^{125}I-labeled hormone was measured using a gamma counter (SN-6105 radioimmunoassay gamma counter; Shanghai Rihuan Photoelectric Instrument, Shanghai, China).

The homeostasis model assessment of insulin resistance (HOMA-IR) was calculated using the following formula: HOMA-IR = fasting insulin (μU/mL) × fasting glucose (mmol/L)/22.5, as described previously (Matthews et al. 1985). The insulin sensitivity index (IAI) was calculated using the formula of IAI = Ln [1/(fasting insulin (μU/mL) × fasting glucose (mmol/L))] (Matsuda and DeFronzo 1999).

GC–MS-based metabolite profiling

Chemicals

All the authentic reference standards and reagents were of analytical, silylation, or chromatography grades as described previously (A et al. 2008). The methoxyamine hydrochloride (purity 98 %), alkane standard solution (C8–C40), pyridine (≥99.8 % GC) and stable isotope-labeled internal standard compound (IS) myristic-1,2-13C2 acid (99 atom % 13C) were provided by Sigma-Aldrich. *N*-methyl-*N*-trimethylsilyltrifluoroacetamide (MSTFA), and 1 % trimethylchlorosilane (TMCS) were provided by Thermo Scientific (Bellefonte, USA). Methanol (high-performance liquid chromatography-grade) and *n*-heptane were provided by Tedia Company (Fairfield, USA) and Merck (Darmstadt, Germany), respectively. All of the aqueous solutions were prepared with pure water produced by a Milli-Q system (Millipore, Bedford, USA).

Sample preparation and GC–MS analysis

The metabolomics approach was presented in Fig. 1. The plasma and urine samples were pretreated, extracted, and derivatized as previously reported (A et al. 2008). Briefly, 50 μL of plasma was added to a tube containing 200 μL of methanol to extract the metabolites and precipitate the protein. [1, 2-^{13}C2]-myristic acid (12.5 μg/mL, Sigma-Aldrich) was added to each tube as the internal standard (IS). One hundred microliter of urine added with 20 Units of urease was incubated at 37 °C for 20 min to decompose and remove excess urea present in it. Then 300 μL methanol (containing internal standard [1, 2-^{13}C2]-myristic acid, 12.5 μg/mL) was added into urinary mixture. The solution was vigorously extracted for 5 min and was centrifuged at 12,000×*g* at 4 °C for 10 min. An aliquot of 100 μL plasma or urinary supernatant was transferred to a GC vial, and then evaporated to dryness using SPD2010-230 SpeedVac Concentrator (Thermo Savant, Holbrook, USA). 30 μL of methoxyamine in pyridine (10 mg/mL, Sigma-Aldrich) was added into the dried extract and vigorously vortex-mixed for 2 min. The methoximation reaction was followed with trimethylsilylation for 1 h by adding 30 μL of MSTFA with 1 % TMCS (Thermo Scientific, Bellefonte, USA) as the catalyst. Finally, the solution was vortex-mixed again for 30 s after the external standard methyl myristate in heptane (30 μg/mL, Merck, Darmstadt, Germany) was added to each GC vial. The metabolites were analyzed by GC–MS system (Shimadzu QP2010Ultra/SE Kyoto, Japan) as described previously (A et al. 2005).

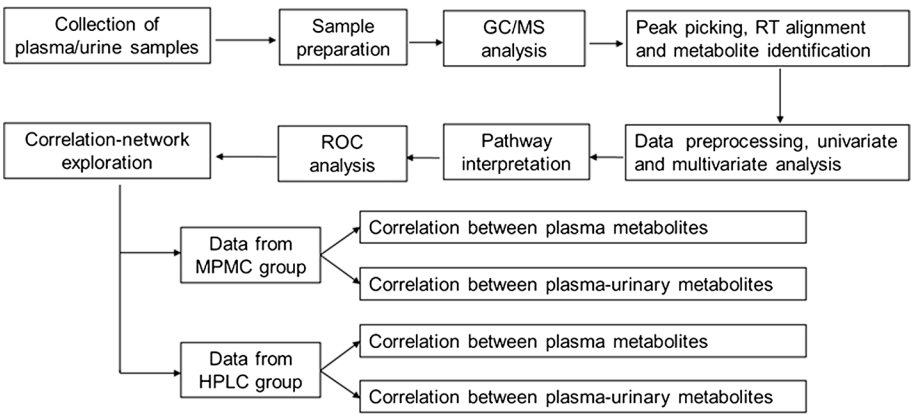

Fig. 1 Outline of the metabolomics approach in the present study

Raw data and data preprocessing

The metabolite peaks were automatically detected, and excluded if the S/N was less than 20. Each of the compound was identified by comparing the mass spectrum and retention index of the analyte with those of reference standards or those available in various libraries, including mainlib and publib in the National Institute of Standards and Technology library 2.0 (NIST 2008) and Wiley 9 (Wiley-VCH Verlag GmbH & Co. KGaA, Weinheim, Germany). To acquire quantitative data, one quant mass was determined according to mass spectrum and the interference from adjacent peaks. The GC/MS spectra were phased and baseline corrected with GCMS solution version 2.6 software (Shimadzu, Kyoto, Japan). The impurity peaks from column bleeds and derivatization procedures were excluded, and the remaining peak areas for each metabolite were normalized against the IS before univariate and multivariate statistical analysis. Before analysis, the repeatability and reproducibility of the method was tested. The relative standard deviation of within-day and between-day precision was less than 3 %. Missing values were assumed to result from areas lower than limits of detection. Thus, the missing values for each metabolite were imputed with the observed minimum after normalization step (Deng et al. 2014).

Multivariate, non-parametric univariate and pathway analysis

The pre-processed GC/MS data were exported into SIMCA-P 13.0 (Umetrics, Umeå, Sweden) for multivariate analysis. The PLS-DA and OPLS-DA analysis were conducted using Pareto-scaled data with sevenfold cross-validation using 200 iterations (Eriksson et al. 2008). The parameters of component number (A), R2X (cum), R2Y (cum) and Q2 (cum) were calculated to describe the quality of a model. OPLS S-plots were separately performed with Pareto-scaled data (Wiklund et al. 2008). The discriminated metabolites are selected based on variable importance in the projection (VIP) value (VIP > 1) from the OPLS-DA model. Different metabolites selected from OPLS-DA analysis were validated using the Wilcoxon–Mann–Whitney test. The false discovery rate (FDR) correction was analyzed with Benjamini–Hochberg adjustments (Benjamini and Hochberg 1995), with the threshold 0.1. Metabolite set enrichment analysis was conducted by using the Metaboanalyst (v 2.0) tool (Xia et al. 2009). The software was used with its default settings, except log-normalization was used for data normalization. The FDR-adjusted $-\log p$ of metabolites were extracted and visualized.

Biomarker identification by receiver operating characteristic curve (ROC) analysis

ROC analysis is generally considered the standard method for describing and assessing the biomarker performance (Obuchowski et al. 2004). To find the biomarker with good discrimination ability between HPLC-fed and MPMC-fed rats, ROC anlaysis was conducted. For potentially clinical application, these markers may be used for discriminating HPLC consumers from MPMC consumers. ROC analysis was conducted with IS-normalized GC/MS data that were VIP selected in OPLS-DA, using the ROCCET web-based tool (Xia et al. 2013). We used the hold-out set ROC curve analysis to test the predictive outcome of certain biomarker. The 5 MPMC and 5 HPLC samples were randomly selected as the training set and the other samples in the two groups were selected among the validation population as the hold-out set. Both individual and multiple biomarker ROC curves were built using the linear support vector machines algorithm. The average of predicted class probabilities of each sample and the average predicted accuracy were then calculated across 100 cross-validations, giving the respective confusion matrices for the training and hold-out sets. The statistical significance of each ROC model was computed using 500 permutation test.

Correlation-network exploration

We sought to detect metabolite correlation that was specifically altered under two diet conditions (MPMC and HPLC). We followed the recommendation by Camacho (Camacho et al. 2005) to conduct the correlation analysis for metabolomics data. The samples in each group (10 replicates) enabled us to analyze the metabolite–metabolite correlation from MPMC or HPLC group, respectively. z value-normalized peak area of each metabolite was used for correlation analysis (Camacho et al. 2005). Spearman correlation coefficients and significances were calculated in XLStat (Addinsoft, Paris, France). Since the topology of correlation network predominantly depends on the chosen correlation threshold, we compared the number of metabolite–metabolite pairs under the p less than 0.05 or 0.01. The number of pair-wise correlation decreased at p 0.05 compared 0.01, for example, number of plasma metabolite–metabolite correlation reduced from 205 to 128. To elucidate the potential systemic property, we focused on the robust correlation of metabolite pairs with p less than 0.01 and Spearman correlation coefficient larger than 0.8, which were subsequently selected for network analysis. The dataset, including pair-wise metabolites with correlation coefficient passing the threshold, were imported into Gephi. Correlation

networks were visualized using the method as described previously (Bastian et al. 2009). A set of measures including network degree, eigenvector centrality, density, were calculated to describe the topology of the resulting network.

Concentration quantification with standards of selected urinary metabolites

Urinary uric acid concentration was determined using the phosphotungstic acid method (Carroll et al. 1971) with uric acid standard. Urinary creatinine concentration was measured by the Jaffe method (Folin 1914). Urinary glucose concentration was determined by the glucose oxidase/peroxidase enzymatic method (Tiffany et al. 1972).

Statistical analysis

Data of body weight, plasma biochemical parameters (metabolites and hormones), urinary uric acid, creatinine, glucose concentration were analyzed by using the non-parametric Mann–Whitney test for independent samples. The data were expressed as mean ± SEM. $p < 0.05$ was considered to indicate statistical significance.

Results

Growth performance and plasma biochemical parameters

Supplementary Table 2 shows the tissue and plasma biochemical parameters measured at the end of the experimental period. HPLC rats had a significantly lower body weight and food intake than MPMC rats (Supplementary Table 2). Since the diets were isoenergetic, the low feed intake led to decreased energy intake in HPLC compared to MPMC rats. Liver weight was significantly reduced in HPLC-fed rats compared to MPMC-fed ones, but spleen weight was no different between the two groups. The weights of mesenteric and epididymal adipose tissue were significantly lower in HPLC-fed rats than in MPMC-fed rats. The relative weight of liver and spleen increased, while the relative weight of mesenteric adipose and epididymal adipose decreased in HPLC compared to MPMC rats. Within the plasma parameters, concentrations of glucose, insulin and triglyceride were reduced, whereas concentrations of urea and high-density lipoprotein cholesterol increased in HPLC compared to MPMC rats. HPLC diet had no significant effect on the level of fasting GPT and GOT compared to MPMC diet. HPLC diet increased the IAI and decreased HOMA-IR compared to MPMC diet.

Table 1 Summary of the model fitness of GC–MS analysis about MPMC and HPLC group

Model	Components[a]	R2Xcum[b]	R2Ycum[c]	Q2cum[d]
Plasma				
PLS-DA	2	0.368	0.934	0.712
OPLS-DA	1P + 1O[e]	0.368	0.933	0.775
Urine				
PLS-DA	3	0.756	0.989	0.916
OPLS-DA	1P + 3O	0.781	0.994	0.957

[a] The number of components used for model analysis

[b,c] R2Xcum and R2Ycum indicate the cumulative sum of squares of all the *X* variations and *Y* variations explained by all extracted components

[d] Q2cum values display the cumulative percent of the variation in *Y* and can be used to estimate how well the model predicts the *Y*

[e] 1P + 1O means one predictive component and one orthogonal component for performing the OPLS-DA analysis

Analysis of plasma and urine metabolites

The GC/MS chromatogram overlay of MPMC and HPLC group rats are shown in Supplementary Fig. 1. GC/MS-based measurement identified 64 metabolites for plasma and 84 metabolites for urine. With multivariate analysis, both the PLS-DA and OPLS-DA models were shown to fit with plasma or urine metabolic profiles (Table 1). For multivariate analysis of plasma metabolites, the goodness of model fit (R2Ycum) was 0.934 and the goodness of prediction (Q2cum) was 0.712 in the PLS-DA model for plasma. The supervised OPLS-DA model showed an R2Ycum of 0.933 and Q2cum of 0.775. For multivariate analysis of urinary metabolites, the PLS-DA model showed the R2Xcum 0.756, R2Ycum 0.989, and Q2cum 0.916 (Table 1). The supervised OPLS-DA analysis showed the R2Xcum 0.781, R2Ycum 0.994, and Q2Ycum 0.957. These results demonstrated a different metabolite composition in the HPLC group compared with the MPMC group.

Plasma metabolites in HPLC-fed rats were characterized by an increase in α-tocopherol, pyruvate, 2-hydroxyisovalerate, BHB, and urea, and a decrease in linoleate, palmitoleate, arachidonate, mannose, alanine, and pyroglutamic acid (Table 2). In plasma, α-tocopherol showed a higher fold change (80.75) in HPLC compared to MPMC rats. Pyruvate and BHB concentrations in HPLC rats increased 2.5-fold, 1.57-fold, respectively, while fatty acids palmitoleate and linoleate decreased 4.1- and 3.65-fold, respectively, compared to MPMC rats. The concentrations of branched amino acid metabolism relatives 2-oxoisocaproate and 2-hydroxyisovalerate were increased in HPLC rats. Based on the relative concentrations of metabolites in plasma, it can be observed that pyruvate metabolism,

Table 2 Significantly altered metabolites in plasma and urine of HPLC compared with MPMC rats

Pathway	Metabolite	Biological roles	Metabolic subpathway	FC[a]	*p* value[b]	FDR *p*[c]	VIP[d]
Plasma metabolites							
Lipid							
	Stearate	Saturated fatty acids	Fatty acid biosynthesis	0.73	0.034	0.099	1.21
	Linoleate	Unsaturated fatty acids	Biosynthesis of unsaturated fatty acids	0.27	<0.001	0.004	1.9
	Palmitate	Saturated fatty acids	Fatty acid biosynthesis	0.46	<0.001	0.004	1.86
	Arachidonate	Unsaturated fatty acids	Biosynthesis of unsaturated fatty acids	0.52	<0.001	0.004	1.84
	Palmitoleate	Unsaturated fatty acids	Fatty acid biosynthesis	0.24	0.001	0.007	1.74
	DHA	Unsaturated fatty acids	Biosynthesis of unsaturated fatty acids	0.54	0.014	0.045	1.37
	Dihydroxybutanoate	Lipid metabolism relatives	Lipid metabolism relatives	1.57	0.002	0.014	1.65
	β-Hydroxybutyrate	Lipid metabolism relatives	Fatty acid beta-oxidation	1.57	0.003	0.018	1.59
	α-Glycerophosphate	Lipid metabolism relatives	Glycerophospholipid metabolism	0.48	0.004	0.021	1.55
Amino acid	Urea	Amino acid metabolism relatives	Ornithine cycle	1.6	<0.001	0.001	2.05
	Alanine	Amino acid	Alanine metabolism	0.63	0.001	0.006	1.77
	Pyroglutamate	Amino acid	Glutathione metabolism	0.72	0.008	0.03	1.46
	2-Oxoisocaproate	Amino acid metabolism relatives	Valine, leucine and isoleucine degradation	1.85	0.027	0.082	1.25
	2-Hydroxyisovalerate	Amino acid metabolism relatives	Others	2.28	0.002	0.017	1.66
Carbohydrate	Mannose	Carbohydrate	Fructose and mannose metabolism	0.79	0.003	0.018	1.58
	Galactose	Carbohydrate	Galactose metabolism	0.56	0.005	0.021	1.54
	Fructose	Carbohydrate	Fructose and mannose degradation	0.48	0.006	0.025	1.5
	Mannonate-gamma-lactone	Carbohydrate	Fructose and mannose metabolism	0.58	0.006	0.025	1.51
Energy	Pyruvate	Organates/carboxylates	TCA cycle	2.5	0.001	0.006	1.79
	Oxalate	Energy-metabolism intermediates	Glyoxylate and dicarboxylate metabolism	1.35	0.011	0.038	1.41
Cofactor/vitamin	α-Tocopherol	Vitamin	Vitamin digestion and absorption	80.75	<0.001	0.004	1.87
Urinary metabolites							
Lipid	2,3-Dihydroxybutanoate	Lipid metabolism relatives	Others	0.17	<0.001	<0.001	1.21
	3,4-Dihydroxybutanoate	Lipid metabolism relatives	Others	0.26	<0.001	<0.001	1.15
	Malonate	Lipid	Beta-alanine metabolism	0.27	<0.001	<0.001	1.39
	Mevalonate	Lipid	Biosynthesis of terpenoids and steroids	0.13	<0.001	<0.001	1.25
	Hydroxyacetate, glycolate	Lipid	Glyoxylate and dicarboxylate metabolism	0.36	<0.001	<0.001	1.2
	2-Quinolinecarboxylate	Lipid	Others	0.32	<0.001	<0.001	1.17
	Glycerate	Lipid	Pentose phosphate pathway	0.37	0.001	0.002	0.99
	5-Hydroxyhexanoate	Lipid	Microbial metabolism	0.49	0.001	0.003	0.98
Amino acid	β-Alanine	Amino acid	Alanine metabolism	0.23	<0.001	<0.001	1.29
	Glycine	Amino acid	Alanine metabolism	0.43	<0.001	0.007	1.22
	Glutamate	Amino acid	Glutamate metabolism	0.56	0.004	0.003	0.95
	L-Threonine	Amino acid	Glycine, serine and threonine metabolism	0.57	0.003	0.003	0.93

Table 2 continued

Pathway	Metabolite	Biological roles	Metabolic subpathway	FC[a]	*p* value[b]	FDR *p*[c]	VIP[d]
	Serine	Amino acid	Glycine, serine and threonine metabolism	0.68	0.013	0.039	0.9
	N-Butyrylglycine	Amino acid metabolism relatives	Others	0.16	<0.001	<0.001	1.23
	Hippurate	Amino acid metabolism relatives	Phenylalanine metabolism	0.19	<0.001	<0.001	1.28
	5-Hydroxyindole	Amino acid metabolism relatives	Others	0.61	<0.001	<0.001	1.23
	Creatinine	Amino acid metabolism relatives	Arginine and proline metabolism	0.34	<0.001	<0.001	1.18
	Tryptophan	Amino acid	Tryptophan metabolism	0.22	<0.001	0.001	1.07
	5-Hydroxyproline	Amino acid	Arginine and proline metabolism	0.49	<0.001	0.001	1.06
	Taurine	Amino acid metabolism relatives	Primary bile acid biosynthesis	0.62	0.001	0.039	1.05
	2-Hydroxyisobutyrate	Amino acid metabolism relatives	Amino acids metabolism relatives	0.52	0.002	0.004	0.95
Carbohydrate	Ribitol	Carbohydrate	Polyol metabolism	0.25	<0.001	<0.001	1.4
	Ribonate	Carbohydrate	Others	0.4	<0.001	0.003	1.33
	Ononitol	Carbohydrate	Polyol metabolism	0.31	<0.001	<0.001	1.3
	Erythro-pentonate	Carbohydrates	Others	0.1	<0.001	<0.001	1.29
	Pentitol	Carbohydrate	Polyol metabolism	0.34	<0.001	<0.001	1.27
	Ribose	Carbohydrate	Pentose phosphate pathway	0.34	<0.001	0.002	1.25
	D-Glucose	Carbohydrate	Glycolysis and gluconeogenesis	0.55	<0.001	0.026	1.22
	Threonate	Carbohydrate	Others	0.4	<0.001	<0.001	1.21
	D-Xylopyranose	Carbohydrate	Others	0.28	<0.001	<0.001	1.2
	Sorbitol	Carbohydrate	Polyol metabolism	0.08	<0.001	<0.001	1.14
	D-Fructose	Carbohydrate	Fructose and mannose degradation	0.28	<0.001	<0.001	1.13
	Erythrose	Carbohydrate/monosaccharide	Others	0.41	<0.001	<0.001	1.19
	Raffinose	Carbohydrate	Galactose metabolism	0.49	<0.001	<0.001	1.1
	Arabinose	Carbohydrate	Pentose and glucuronate interconversions	0.09	<0.001	<0.001	1.09
	Glucuronate	Carbohydrate/monosaccharide	Starch and sucrose metabolism	0.62	<0.001	0.058	1.06
	N-Acetyl glucosamine	Carbohydrates/monosaccharides	Galactose metabolism	0.42	<0.001	0.001	1.05
	2,3-Butanediol	Carbohydrate/alkaloid	Butanoate metabolism	0.74	0.001	0.001	1.04
Cofactor/vitamin	Pantothenate	Cofactors/vitamins	Pantothenate and CoA Biosynthesis	0.23	<0.001	<0.001	1.22
	Ascorbate	Cofactors/vitamins	Ascorbate and aldarate metabolism	0.27	<0.001	<0.001	1.22
Energy	Aconitate	Organates/carboxylates	TCA cycle	0.16	<0.001	<0.001	1.3
	Citrate	Organate/carboxylate	TCA cycle	0.08	<0.001	<0.001	1.19
	Pyruvate	Organates/carboxylates	TCA cycle	0.38	<0.001	<0.001	1.14
	Malate	Organates/carboxylates	Glycolysis and gluconeogenesis	0.4	<0.001	<0.001	1.09
	Succinate	Organates	TCA cycle	0.17	<0.001	<0.001	1.12

Table 2 continued

Pathway	Metabolite	Biological roles	Metabolic subpathway	FC[a]	*p* value[b]	FDR *p*[c]	VIP[d]
Nucleotide	Pseudo uridine	Nucleate	Pyrimidine metabolism	0.31	<0.001	<0.001	1.19
	Uridine	Nucleate	Pyrimidine metabolism	0.39	<0.001	<0.001	1.23
	Allantoin	Nucleate relatives	Purine metabolism	0.42	<0.001	<0.001	1.25
	3-Hydroxypyridine	Nucleate	Nicotinate and nicotinamide metabolism	0.53	<0.001	<0.001	1.16
	Urate	Nucleate relatives	Purine metabolism	0.38	<0.001	<0.001	1.11
Others	3,4,5-Trihydroxypentanoate	Organates	Others	0.37	<0.001	<0.001	1.13

[a] FC, fold change for concentration of metabolites derived from HPLC compared with MPMC

[b] The significance *p* value was obtained from Wilcoxon–Mann–Whitney test with the threshold 0.05

[c] Metabolites with the false discovery ratio less than 0.1

[d] VIP value was obtained from OPLS-DA model with a threshold of 1.0

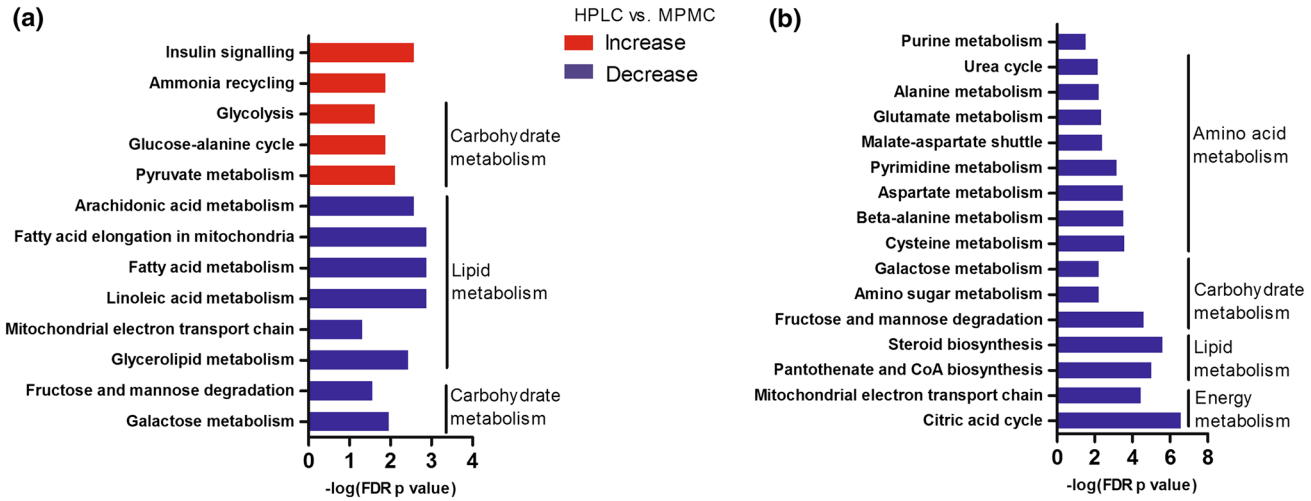

Fig. 2 Pathway analysis of plasma (**a**) and urine (**b**) metabolites. *X*-axis indicates the FDR-adjusted *p* value

ammonia recycling, and fatty acid metabolism were significantly affected by HPLC diet (Fig. 2a).

Urinary metabolites in the HPLC group were characterized with higher concentrations of stearate and palmitate, and lower concentrations of allantoin, citrate, sorbitol, arabinose, hippurate, 2-ketoglutarate, mevalonate, erythro-pentonate, and tryptophan than those in MPMC rats (Table 2). In urine, concentrations of many metabolites involved in AA and carbohydrate metabolism were significantly decreased in the HPLC group. Citrate, sorbitol, arabinose, and erythro-pentonate showed an apparent reduction in HPLC rats with a fold change <0.13 compared to MPMC-fed rats, suggesting that these four metabolites might be sensitive to a HPLC diet-induced metabolic effect. The relative concentration of BHB was decreased in urine of HPLC compared to MPMC rats. Quantitative concentrations of urinary metabolites (glucose, uric acid, creatinine) were consistent with the GC/MS results (Supplementary Table 3). For pathway analysis of urinary metabolites, metabolic pathways, including the TCA cycle, alanine, aspartate and glutamate metabolism, and steroid biosynthesis showed significant alteration (Fig. 2b). As shown by the pathway results, HPLC diet significantly affected system metabolism compared to the MPMC diet.

Metabolite markers associated with the level of protein intake

We tested a combination of plasma urea and pyruvate, the two candidate biomarkers commercially available. The result of plasma urea and pyruvate combination is shown in Fig. 3. The results obtained with the validation population

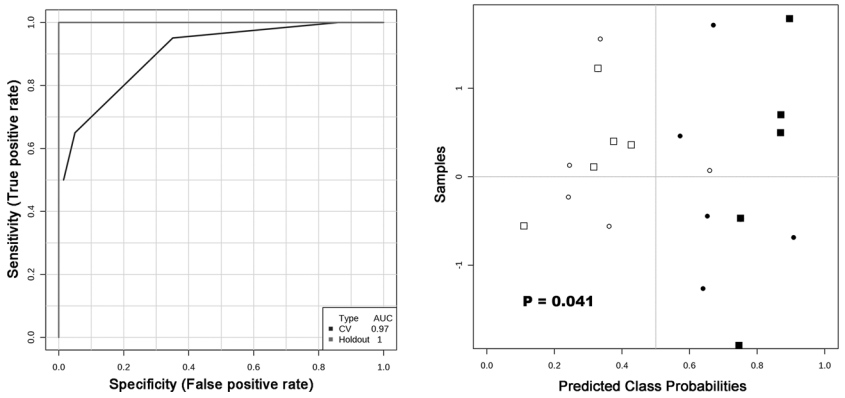

Confusion matrix (cross-validation)		
	MPMC consumers	HPLC consumers
Predicted MPMC intake	4	0
Predicted HPLC intake	1	5
Confusion matrix (hold-out)		
	MPMC consumers	HPLC consumers
Predicted MPMC intake	5	0
Predicted HPLC intake	0	5

Fig. 3 ROC curve analysis of plasma urea in combination with pyruvate. *Left figure*, *black curves* represent the training set ($n = 10$ from each group) and *gray curves* the hold-out set ($n = 10$ from each group). *Middle figure* probabilities of predicted belonging to the high consumer class. Training set, *black plots*; hold-out set, *square plots*; *filled circles* HPLC rats; *empty circles* MPMC rats. *Right figure* confusion matrices for the two datasets

confirmed that the combination of urea and pyruvate in plasma yielded excellent discrimination of HPLC from MPMC group (AUC 1.0). The average accuracy based on 100 cross-validations is 0.855. The accuracy for hold-out data prediction is 1(10/10). Furthermore, the results of the permutation test ($n = 500$) showed that the model based on urea–pyruvate combination is significant ($p = 0.041$), whereas the urea-based model is not ($p = 0.10$). The urinary citrate-based model also yielded excellent predictive accuracy (AUC 1, $p = 0.036$). A combination of urinary pyruvate and creatinine also yielded excellent predictive accuracy (AUC 0.98, $p = 0.031$).

Network descriptions

We constructed the plasma metabolite correlation network using data from the MPMC and HPLC groups (Fig. 4). The degree of a vertex of a graph is the number of edges incident on the vertex. The density represents how tightly co-related a set of nodes is within a module. Eigenvector centrality assigns relative scores to all nodes in the network based on the concept that connections to high-scoring nodes contribute more to the score of the node in question than equal connections to low-scoring nodes (Noguchi et al. 2008).

The network degree and density were increased in HPLC rats compared to MPMC group (0.06 vs. 0.035, 3.607 vs. 2.098, respectively) (Fig. 4a), suggesting that the HPLC diet increased the plasma metabolite pair-wise correlation linkage compared to the MPMC diet. The correlation between plasma AA and energy-metabolism relatives was stronger in HPLC rats than in the MPMC group. For example, the energy-metabolism relatives 2-ketoglutarate, fumarate, and malate were positively correlated with phenylalanine, methionine, and serine (Supplementary Fig. 2a). The connection between AAs increased in the HPLC group (Supplementary Fig. 2b). Supplementary Table 4 shows the different network indices of plasma metabolites in the MPMC and HPLC groups. Among the plasma metabolites of MPMC rats, uric acid had the highest eigenvector centrality (1) and degree (6), followed by glutamine and lactate. Among the plasma metabolites of HPLC rats, alanine had the highest eigenvector centrality (1) and degree (13), and 9 of the top 10 metabolites with high eigenvector centrality were AAs. The eigenvector centrality and degree of fumarate, an energy-metabolism relative, increased in the HPLC group compared to the MPMC group (0.74 vs. 0.04 and 10 vs. 2). The eigenvector centrality of AA metabolism relatives (β-amino isobutyrate, glycine, isoleucine, lysine, methionine, phenylalanine and proline) was higher in the correlation network of HPLC group than in the MPMC group. These results suggested that the pair-wise correlation network of plasma metabolites shifted and increased after HPLC intake.

The network of correlations between urine and plasma metabolites was also constructed (Supplementary Fig. 3). In the network of plasma–urine metabolites of the MPMC group, plasma valine had the highest betweenness centrality (52.5), degree (9), and eigenvector centrality (1) (Supplementary Table 5). These three parameters of valine surpassed all other metabolites in their connection numbers. Plasma pyruvate exhibited the secondary betweenness centrality (27) and degree (6) in the plasma–urine metabolites of the MPMC group. In the network of plasma–urine metabolites, plasma 2-oxoisocaproate showed a relatively higher degree than BHB in the plasma metabolites of HPLC-fed rats (Supplementary Table 5).

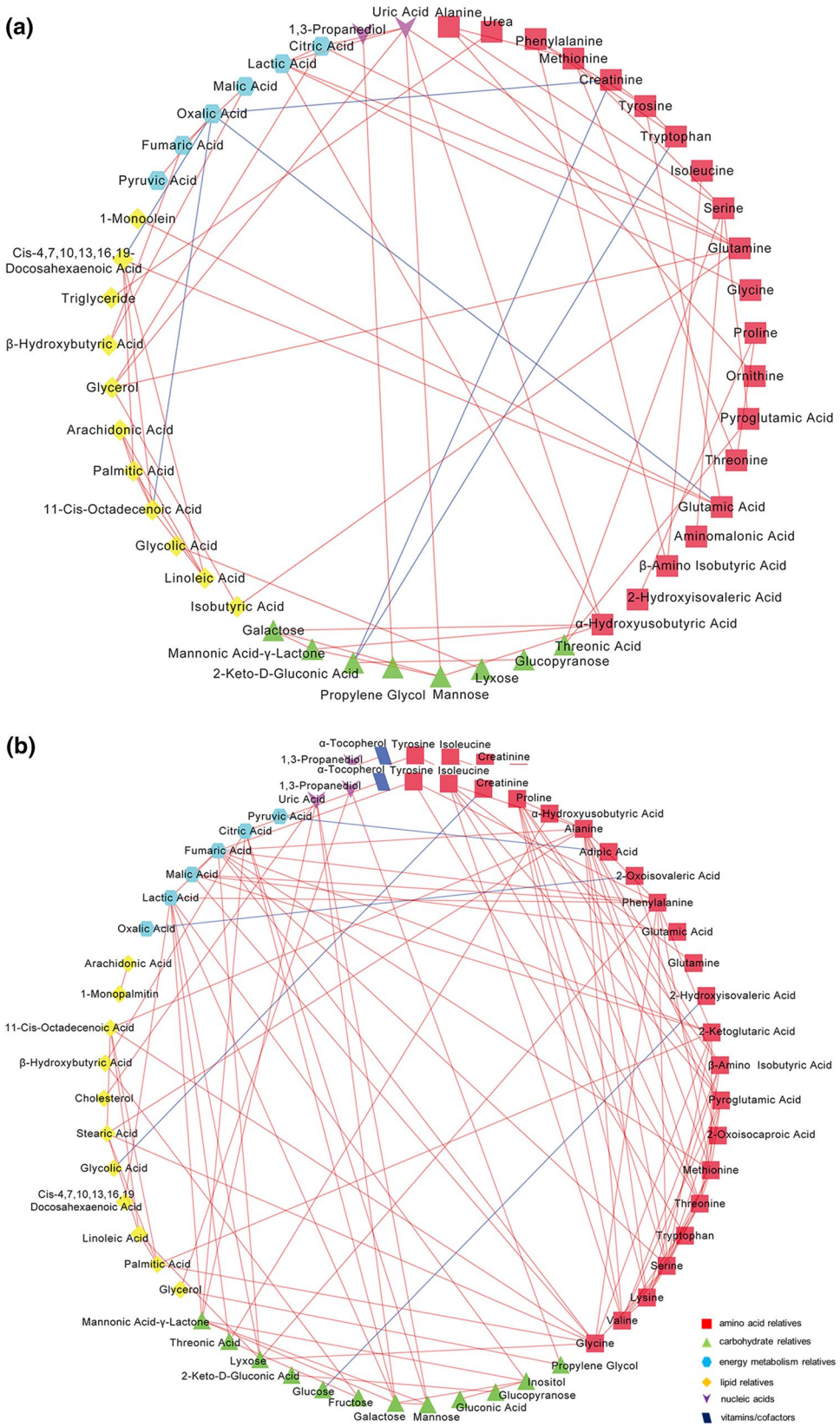

Fig. 4 Plasma metabolite pair-wise correlation network using data from MPMC (**a**) and HPLC (**b**) group. The *blue line* between two metabolites indicated negative correlation and *red line* indicated positive correlation. Correlations with p value less than 0.01 and coefficient more than 0.8 were used to construct the network (color figure online)

Discussion

In the present study, an integrated approach, including GC/MS-based metabolomics profiling and correlation network analysis, was adopted, and for the first time, enabled biochemical metabolism in MPMC and HPLC rats to be revealed. In agreement with previous studies (Chevalier et al. 2013; Jean et al. 2001; Lacroix et al. 2004), our research demonstrated some hyperproteic diet-related changes, including persistent weight loss and lower food intake, an obvious reduction of plasma triglyceride and adipose tissue weight, and a decrease of plasma glucose and insulin in HPLC compared to MPMC rats. Thus, these parameters could be seen as phenotypes that can provide a reference for the application of nutrient interventions by protein supplement against hyperglycemia and hypercholesteremia.

An obvious diet-responsive alteration is the elevation of concentration of plasma urea. Excessive protein intake could possibly increase AA deamination in the liver, and thus induce urea synthesis (Stepien et al. 2011). Another apparent diet-responsive alteration is the increase in α-tocopherol in plasma with an HPLC diet. α-Tocopherol possesses an anti-oxidation function and can enter the plasma from gut to liver by combining with VLDL. Previous studies have shown that a diet high in casein may result in oxidative damage by increasing the contents of superoxide anion and malondialdehyde and decreasing activities of super oxide dismutase and glutathione peroxidase (Gu et al. 2008). Thus, the increase of α-tocopherol after high-protein intake in the present study may help HPLC-fed rats to counteract the pro-oxidation of a high casein diet in the present study.

Energy metabolism

Metabolomics profiling analysis showed that HPLC feeding exerted influence on many metabolism pathways in rats (Fig. 2). One novel finding from this metabolic profiling in the present study is the impact of the HPLC diet on the TCA cycle. According to pathway analysis of urinary metabolites, the TCA cycle was among the most affected pathways. This was evident by the decrease in relative concentrations of urinary citrate, succinate, aconitate, and malate. Although the concentration of urinary TCA metabolites decreased (Table 2), the local TCA cycle was not altered, as reflected by plasma metabolite analysis (Fig. 2). Since urinary metabolites contain molecules that have participated in the whole body's metabolic circulation, the decrease in urinary TCA intermediates may be related to weight loss in HPLC rats. On the other hand, the similar concentration of TCA metabolites between MPMC and HPLC group in plasma may be associated with AAs. This could be reflected by the increase in the positive correlation between energy-metabolism relatives with some carbohydrates (mannose, galactose) or other AA (phenylalanine, methionine, serine) in HPLC rats. The correlation of energy-metabolism relatives with AA may be explained in that the increase in dietary protein gave rise to the utilization of AA by AA oxidation and the Stickland reaction (Jean et al. 2001; Lacroix et al. 2004). The AA deamination process provided carbon skeleton intermediates for the TCA cycle and gluconeogenesis, thereby producing partial energy for the host.

Branched-chain amino acids metabolism

BCAAs could be catabolized to contribute carbon skeletons to the TCA cycle for energy production. The plasma metabolites that are associated with BCAA metabolism (2-hydroxyisovalerate, 2-oxoisocaproate) were increased in HPLC-fed rats, suggesting the upregulation of BCAA metabolism, which was consistent with the previous research conducted in high protein-fed cats (Deng et al. 2014). Valine was converted to 2-oxoisovalerate and metabolized to succinyl-CoA or acetyl-CoA, which participated in the TCA cycle or ketone body biosynthesis (Huang et al. 2011). By correlation network analysis, a negative correlation between plasma valine and urinary ketone bodies (BHB and 2,3-dihydroxybutyrate) was found in the normal MPMC rats, which indicated that the valine may be preferential to enter into the TCA cycle rather than ketone body biosynthesis. However, the HPLC diet changed the correlation network of plasma–urinary metabolites, where the correlation of plasma valine with urinary metabolites decreased but the plasma 2-oxoisocaproate showed a correlation with several urinary metabolites. Plasma valine and 2-oxoisocaproate showed negative correlations with raffinose under MPMC and HPLC conditions, respectively. Although there is no direct relationship between BCAA metabolism and raffinose metabolism, the TCA cycle may link them through acetyl-CoA. Generally, correlation networks tend to show many correlations between metabolites that are biologically disconnected. It is difficult to interpret the exact implication of these correlations. Nevertheless, many statistical-based correlations in the present study could provide new insights into our understanding of the complexity of the metabolic network.

Carbohydrate metabolism

Glucose oxidation is a major pathway that gives rise to acetyl-CoA for the TCA cycle. In the present study, glucose oxidation was relatively increased, as shown by plasma metabolites (decrease in glucose and increase in pyruvate concentration). Pyruvate was an important pivot and

indicator for central energy metabolism. One novel finding is that plasma pyruvate was increased in HPLC rats, while the urinary pyruvate concentration was relatively decreased (Table 2). This contradictory effect of HPLC intake on plasma and urine, as reflected by the increased pyruvate uptake compared to secretion, may be partially due to the increased energy requirement in HPLC-fed rats. Meanwhile, the concentration of lactate, an anaerobic glycolysis product, was similar in the MPMC and HPLC groups. The elevated glucose oxidation in HPLC-fed rats may serve as an alternative pathway to fulfill their decreased energy supply. Pantothenate plays a positive role in fatty acid metabolism and facilitates acetyl-CoA entry into the TCA cycle (Qi et al. 2012). The current study showed the relative concentration of urinary pantothenate was significantly decreased in HPLC-fed rats. Thus, the low concentration of urinary TCA metabolites and pantothenate in HPLC-fed rats in comparison with MPMC-fed rats suggested that the significant effect of the HPLC diet on TCA function may be pantothenate-associated.

Lipid metabolism

Our findings from the metabolomics profiles further showed that lipid anabolism and β-oxidation were largely affected by the HPLC diet. In accordance with previous research (Jean et al. 2001), an obvious reduction of adipose weight due to HPLC ingestion was observed in the current study. In the current study, the concentration of some fatty acid biosynthesis relatives, including plasma α-glycerophosphate, triglyceride, and some fatty acids, were significantly decreased, indicating their important role in the reduction of adipose weight and fatty acid biosynthesis. Our results showed a clear change in lipid β-oxidation after HPLC intake. The concentration of β-oxidation products, namely BHB and dihydroxybutyrate, was increased in plasma, indicating the upregulation of ketogenesis. This was in accordance with previous study that high AA intake increased the carbon skeleton for acetyl-CoA and BHB production (Schwarz et al. 2012). BHB serves as an important ketone body for energy utilization and food control (Johnstone et al. 2008). Thus, the increase of β-oxidation products in the present study possibly indicated the active fatty acid β-oxidation process in liver metabolism. Since BHB may be also involved in the increased glutathione synthesis in liver (Jarrett et al. 2008), the increase in BHB may protect the HPLC rats from oxidative stress. Combined with the findings on glucose and BCAA metabolism, we found the increase in glucose oxidation, lipid oxidation, and BCAA degradation, which produced the acetyl-CoA (Fig. 5). The acetyl-CoA may be involved in the increased ketogenesis that promoted energy metabolism. On the other hand, acetyl-CoA could also be used for lipogenesis. The decrease in lipogenesis under HPLC diet may increase the acetyl-CoA utilization into energy metabolism. Therefore, the potential competition between AA, glucose, lipid metabolism under HPLC diet may be that acetyl-CoA may promote energy metabolism but not lipogenesis. These findings from metabolomics analysis could further help our understanding of HPLC-associated metabolic alteration.

In terms of metabolic syndrome risk or prevention, HPLC diet could increase insulin sensitivity (Supplementary Table 2), which was in accordance with previous research that the increased protein:carbohydrate ratio in diet was related to the improved insulin sensitivity in rats (Blouet et al. 2006). Roberts et al. (2014) and Menni et al. (2013) suggested that the increase in BCAA degradation product (such as 2-oxoisocaproate) may indicate impaired glucose tolerance, which was associated with type 2 diabetes. In the present study, the increase in 2-oxoisocaproate and BHB after HPLC diet may be related to the increased amino acid intake. Some clinical researches have also showed that high-protein diet improved glycaemic control in human subjects with type 2 diabetes mellitus (Gannon et al. 2003; Layman et al. 2008). Therefore, HPLC diet may be beneficial for individuals with impaired glucose tolerance. In contrast, we found that HPLC may be disadvantageous to renal function and muscle metabolism. The significant reduction in urinary creatinine and taurine were related to lower muscular activity and creatine phosphate storage. Urinary allantoin level serves as an indicator for renal glomerular filtration rate (Salek et al. 2007). The low concentration of allantoin in HPLC rats may be associated with reduced renal glomerular filtration rate. As indicated earlier, high-protein diet may reduce bone density and have adverse effects on kidney function (Clifton 2012). Therefore, HPLC diet may be detrimental to peoples with kidney disease.

Correlation network

In the present study, advanced metabolomics techniques enabled the correlation network of metabolomics profiles to be revealed. The metabolomics profiling showed two distinct correlation networks in MPMC and HPLC rats, which may further suggest a metabolic shift after HPLC diet. An increased dense linkage with HPLC diet may suggest an enhanced metabolic connection with HPLC diet. Pair-wise correlations of plasma AA-metabolism relatives existed both in MPMC and HPLC rats (Fig. 4), which reflects the fact that metabolites with similar properties and functions are related to each other (Steuer 2006). Our findings further showed that the metabolic response to HPLC intake was not just limited to the change of concentrations of individual metabolites, but also accompanied with changes in metabolite correlations. Using the theory of stochastic systems and

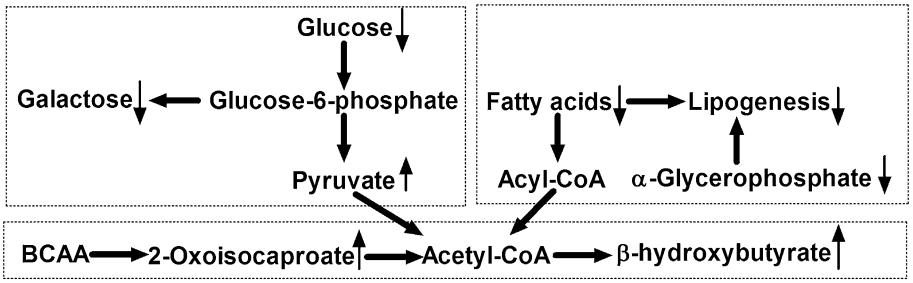

Fig. 5 Proposed metabolic map from plasma metabolite analysis. *Up arrow* indicated the metabolite was increased in HPLC vs. MPMC rats, and *down arrow* indicated the metabolite was decreased in HPLC vs. MPMC rats

metabolic control (such as metabolic co-response profiles), Camacho et al. (2005) and Steuer et al. (2006) found that chemical equilibrium, mass conservation, and asymmetric control serve as important factors that could lead to a high correlation between two metabolites. Thus, the present networking approach may provide new framework for future research on potential metabolic pathways based on metabolite correlations.

Conclusions

The present study provided the first account of the systemic metabolic response to dietary protein/carbohydrate level in a rat model by integrating GC/MS-based metabolomics profiling and correlation network analysis. Potential biomarkers were identified for HPLC intervention, such as plasma urea and pyruvate, and urinary citrate. Correlation network analysis revealed distinguishing patterns in intrinsic metabolite correlations between MPMC and HPLC diets. The plasma metabolite correlation in HPLC rats was increased with energy-metabolism intermediates densely correlated with AAs. Plasma BCAA relatives valine and 2-oxoisocaproate showed negative correlations with some urinary metabolites in MPMC and HPLC rats, respectively. Although HPLC diet decreased body weight and increased insulin sensitivity, it may affect the muscle metabolism and renal function. Thus, a moderate amount of protein intake may confer more benefit for body weight and glycaemic control. These findings provided new insights into our understanding of the mechanisms involved in systemic metabolic regulation in response to dietary protein/carbohydrate level, and this approach may provide a new framework for future studies to evaluate the impact of dietary intervention on animal and human nutrition and health.

Acknowledgments This work was supported by the National Key Basic Research Program of China (2013CB127300), Natural Science Foundation of China (31430082) and Jiangsu Province Natural Science Foundation (BK20130058).

Conflict of interest The authors declare no competing financial interest.

References

A J, Trygg J, Gullberg J, Johansson AI, Jonsson P, Antti H, Marklund SL, Moritz T (2005) Extraction and GC/MS analysis of the human blood plasma metabolome. Anal Chem 77:8086–8094

A J, Huang Q, Wang G, Zha W, Yan B, Ren H, Gu S, Zhang Y, Zhang Q, Shao F, Sheng L, Sun J (2008) Global analysis of metabolites in rat and human urine based on gas chromatography/time-of-flight mass spectrometry. Anal Biochem 379:20–26

Bastian M, Heymann S, Jacomy M (2009) Gephi: an open source software for exploring and manipulating networks. ICWSM 8:361–362

Benjamini Y, Hochberg Y (1995) Controlling the false discovery rate—a practical and powerful approach to multiple testing. J Roy Stat Soc B Met 57:289–300

Blouet C, Mariotti F, Azzout-Marniche D, Bos C, Mathe V, Tome D, Huneau JF (2006) The reduced energy intake of rats fed a high-protein low-carbohydrate diet explains the lower fat deposition, but macronutrient substitution accounts for the improved glycemic control. J Nutr 136:1849–1854

Camacho D, de la Fuente A, Mendes P (2005) The origin of correlations in metabolomics data. Metabolomics 1:53–63

Carroll JJ, Coburn H, Douglass R, Babson AL (1971) A simplified alkaline phosphotungstate assay for uric acid in serum. Clin Chem 17:158–160

Chevalier L, Bos C, Azzout-Marniche D, Fromentin G, Mosoni L, Hafnaoui N, Piedcoq J, Tome D, Gaudichon C (2013) Energy restriction only slightly influences protein metabolism in obese rats, whatever the level of protein and its source in the diet. Int J Obes 37:263–271

Clifton P (2012) Effects of a high protein diet on body weight and comorbidities associated with obesity. Brit J Nutr 108:S122–S129

Deng P, Jones JC, Swanson KS (2014) Effects of dietary macronutrient composition on the fasted plasma metabolome of healthy adult cats. Metabolomics 10:638–650

Eriksson L, Trygg J, Wold S (2008) CV-ANOVA for significance testing of PLS and OPLS® models. J Chemom 22:594–600

Folin O (1914) On the determination of creatinine and creatine in urine. J Biol Chem 17:469–473

Gannon MC, Nuttall FQ, Saeed A, Jordan K, Hoover H (2003) An increase in dietary protein improves the blood glucose response in persons with type 2 diabetes. Am J Clin Nutr 78:734–741

Gu C, Shi Y, Le G (2008) Effect of dietary protein level and origin on the redox status in the digestive tract of mice. Int J Mol Sci 9:464–475

Halton TL, Hu FB (2004) The effects of high protein diets on thermogenesis, satiety and weight loss: a critical review. J Am Coll Nutr 23:373–385

Huang Y, Zhou M, Sun H, Wang Y (2011) Branched-chain amino acid metabolism in heart disease: an epiphenomenon or a real culprit? Cardiovasc Res 90:220–223

Jarrett SG, Milder JB, Liang LP, Patel M (2008) The ketogenic diet increases mitochondrial glutathione levels. J Neurochem 106:1044–1051

Jean C, Rome S, Mathe V, Huneau JF, Aattouri N, Fromentin G, Achagiotis CL, Tome D (2001) Metabolic evidence for adaptation to a high protein diet in rats. J Nutr 131:91–98

Johnstone AM, Horgan GW, Murison SD, Bremner DM, Lobley GE (2008) Effects of a high-protein ketogenic diet on hunger, appetite, and weight loss in obese men feeding ad libitum. Am J Clin Nutr 87:44–55

Lacroix M, Gaudichon C, Martin A, Morens C, Mathe V, Tome D, Huneau JF (2004) A long-term high-protein diet markedly reduces adipose tissue without major side effects in Wistar male rats. Am J Physiol-Reg I 287:R934–R942

Layman DK, Clifton P, Gannon MC, Krauss RM, Nuttall FQ (2008) Protein in optimal health: heart disease and type 2 diabetes. Am J Clin Nutr 87:1571s–1575s

Matsuda M, DeFronzo RA (1999) Insulin sensitivity indices obtained from oral glucose tolerance testing—comparison with the euglycemic insulin clamp. Diabetes Care 22:1462–1470

Matthews D, Hosker J, Rudenski A, Naylor B, Treacher D, Turner R (1985) Homeostasis model assessment: insulin resistance and β-cell function from fasting plasma glucose and insulin concentrations in man. Diabetologia 28:412–419

Menni C, Fauman E, Erte I, Perry JRB, Kastenmuller G, Shin SY, Petersen AK, Hyde C, Psatha M, Ward KJ, Yuan W, Milburn M, Palmer CNA, Frayling TM, Trimmer J, Bell JT, Gieger C, Mohney RP, Brosnan MJ, Suhre K, Soranzo N, Spector TD (2013) Biomarkers for type 2 diabetes and impaired fasting glucose using a nontargeted metabolomics approach. Diabetes 62:4270–4276

Nicholson JK, Holmes E, Kinross JM, Darzi AW, Takats Z, Lindon JC (2012) Metabolic phenotyping in clinical and surgical environments. Nature 491:384–392

Noguchi Y, Shikata N, Furuhata Y, Kimura T, Takahashi M (2008) Characterization of dietary protein-dependent amino acid metabolism by linking free amino acids with transcriptional profiles through analysis of correlation. Physiol Genomics 34:315–326

Obuchowski NA, Lieber ML, Wians FH (2004) ROC curves in clinical chemistry: uses, misuses, and possible solutions. Clin Chem 50:1118–1125

Qi Y, Li P, Zhang YY, Cui LL, Guo Z, Xie GX, Su MM, Li X, Zheng XJ, Qiu YP, Liu YM, Zhao AH, Jia WP, Jia W (2012) Urinary metabolite markers of precocious puberty. Mol Cell Proteomics 11(1):M111.011072

Rasmussen LG, Winning H, Savorani F, Toft H, Larsen TM, Dragsted LO, Astrup A, Engelsen SB (2012) Assessment of the effect of high or low protein diet on the human urine metabolome as measured by NMR. Nutrients 4:112–131

Reimer RA, Maurer AD, Eller LK, Hallam MC, Shaykhutdinov R, Vogel HJ, Weljie AM (2012) Satiety hormone and metabolomic response to an intermittent high energy diet differs in rats consuming long-term diets high in protein or prebiotic fiber. J Proteome Res 11:4065–4074

Reitman S, Frankel S (1957) A colorimetric method for the determination of Serum glutamate pyruvate transaminase and serum glutamate oxaloacetate transaminase. Am J Clin Path 28:56–62

Roberts LD, Koulman A, Griffin JL (2014) Towards metabolic biomarkers of insulin resistance and type 2 diabetes: progress from the metabolome. Lancet Diabetes Endo 2:65–75

Ross AB, Pere-Trepat E, Montoliu I, Martin FPJ, Collino S, Moco S, Godin JP, Cleroux M, Guy PA, Breton I, Bibiloni R, Thorimbert A, Tavazzi I, Tornier L, Bebuis A, Bruce SJ, Beaumont M, Fay LB, Kochhar S (2013) A whole-grain-rich diet reduces urinary excretion of markers of protein catabolism and gut microbiota metabolism in healthy men after one week. J Nutr 143:766–773

Russell WR, Gratz SW, Duncan SH, Holtrop G, Ince J, Scobbie L, Duncan G, Johnstone AM, Lobley GE, Wallace RJ, Duthie GG, Flint HJ (2011) High-protein, reduced-carbohydrate weight-loss diets promote metabolite profiles likely to be detrimental to colonic health. Am J Clin Nutr 93:1062–1072

Sacks FM, Bray GA, Carey VJ, Smith SR, Ryan DH, Anton SD, McManus K, Champagne CM, Bishop LM, Laranjo N, Leboff MS, Rood JC, de Jonge L, Greenway FL, Loria CM, Obarzanek E, Williamson DA (2009) Comparison of weight-loss diets with different compositions of fat, protein, and carbohydrates. New Engl J Med 360:859–873

Salek RM, Maguire ML, Bentley E, Rubtsov DV, Hough T, Cheeseman M, Nunez D, Sweatman BC, Haselden JN, Cox RD, Connor SC, Griffin JL (2007) A metabolomic comparison of urinary changes in type 2 diabetes in mouse, rat, and human. Physiol Genomics 29:99–108

Schicho R, Shaykhutdinov R, Ngo J, Nazyrova A, Schneider C, Panaccione R, Kaplan GG, Vogel HJ, Storr M (2012) Quantitative metabolomic profiling of serum, plasma, and urine by H-1 NMR spectroscopy discriminates between patients with inflammatory bowel disease and healthy individuals. J Proteome Res 11:3344–3357

Schwarz J, Tome D, Baars A, Hooiveld GJEJ, Muller M (2012) Dietary protein affects gene expression and prevents lipid accumulation in the liver in mice. Plos One 7:e47303

Seyfried F, Li JV, Miras AD, Cluny NL, Lannoo M, Fenske WK, Sharkey KA, Nicholson JK, le Roux CW, Holmes E (2013) Urinary Phenotyping indicates weight loss-independent metabolic effects of Roux-en-Y gastric bypass in mice. J Proteome Res 12:1245–1253

Solon-Biet SM, McMahon AC, Ballard JW, Ruohonen K, Wu LE, Cogger VC, Warren A, Huang X, Pichaud N, Melvin RG, Gokarn R, Khalil M, Turner N, Cooney GJ, Sinclair DA, Raubenheimer D, Le Couteur DG, Simpson SJ (2014) The ratio of macronutrients, not caloric intake, dictates cardiometabolic health, aging, and longevity in ad libitum-fed mice. Cell Metab 19:418–430

Stepien M, Gaudichon C, Fromentin G, Even P, Tome D, Azzout-Marniche D (2011) Increasing protein at the expense of carbohydrate in the diet down-regulates glucose utilization as glucose sparing effect in rats. Plos One 6:e14664

Steuer R (2006) Review: on the analysis and interpretation of correlations in metabolomic data. Brief Bioinform 7:151–158

Tiffany T, Jansen J, Burtis C, Overton J, Scott C (1972) Enzymatic kinetic rate and end-point analyses of substrate, by use of a GeMSAEC fast analyzer. Clin Chem 18:829–840

Wiklund S, Johansson E, Sjostrom L, Mellerowicz EJ, Edlund U, Shockcor JP, Gottfries J, Moritz T, Trygg J (2008) Visualization of GC/TOF-MS-based metabolomics data for identification of biochemically interesting compounds using OPLS class models. Anal Chem 80:115–122

Xia JG, Psychogios N, Young N, Wishart DS (2009) MetaboAnalyst: a web server for metabolomic data analysis and interpretation. Nucleic Acids Res 37:W652–W660

Xia JG, Broadhurst DI, Wilson M, Wishart DS (2013) Translational biomarker discovery in clinical metabolomics: an introductory tutorial. Metabolomics 9:280–299